JUSTC
Article
http://justc.ustc.edu.cn
Received: December 10, 2024; Accepted: March 06, 2025

Realizing soft two-dimensional room temperature magnets in oxidized $(Fe_{75}Co_{25})_5GeTe_2$

Chunyu Qin[1], Yanan Yuan[1], Jiapeng Zhao[2], Daxiang Liu[1], Fangfang Pei[1], Siyu Wang[1], Xiaoli Chen[1], Xiang Chen[3], Hongrui Zhang[4], Mengmeng Yang[5], He Huang[2] ✉, and Qian Li[1] ✉

[1]*National Synchrotron Radiation Laboratory, and School of Nuclear Science and Technology, University of Science and Technology of China, Hefei 230029, China;*
[2]*School of Materials Science and Engineering, University of Science and Technology Beijing, Beijing 100083, China;*
[3]*Center for Neutron Science and Technology, Guangdong Provincial Key Laboratory of Magnetoelectric Physics and Devices, School of Physics, Sun Yat-Sen University, Guangzhou 510275, China;*
[4]*Ningbo Institute of Materials Technology & Engineering, Chinese Academy of Sciences, Ningbo 315201, China;*
[5]*Anhui Key Laboratory of Magnetic Functional Materials and Devices, Institute of Physical Science and Information Technology, Anhui University, Hefei 230601, China*

✉Correspondence: He Huang, E-mail: hhuang@ustb.edu.cn; Qian Li, E-mail: liqian89@ustc.edu.cn

Graphical abstract

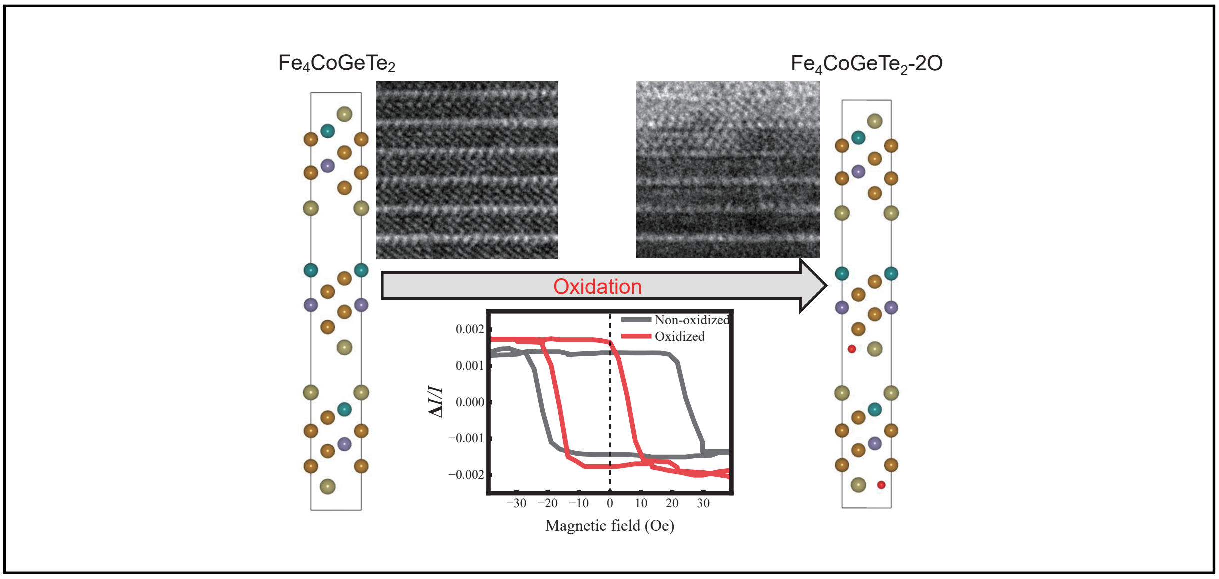

Differences in the $(Fe_{75}Co_{25})_5GeTe_2$ flake before and after oxidation.

Public summary

■ The successful fabrication and characterization of high-quality $(Fe_{75}Co_{25})_5GeTe_2$ room-temperature van der Waals ferromagnetics are presented.

■ A small coercivity (~3 Oe) and low damping (~0.040) at room temperature in $(Fe_{75}Co_{25})_5GeTe_2$ were reported, indicating that this material is an ideal soft in-plane room temperature 2D magnet used in future 2D magnet-based spintronic devices.

■ Compared with the freshly exfoliated sample, the oxidized $(Fe_{75}Co_{25})_5GeTe_2$ sample exhibited exchange bias and smaller coercivity, demonstrating that the oxidation strategy is an effective method for modulating the magnetic properties of 2D magnets.

Citation: Qin C Y, Yuan Y N, Zhao J P, et al. Realizing soft two-dimensional room temperature magnets in oxidized $(Fe_{75}Co_{25})_5GeTe_2$. *JUSTC*, **2025**, 55(10): 1004. CSTR: 32290.14.JUSTC-2024-0153. DOI: 10.52396/JUSTC-2024-0153

JUSTC
Article
http://justc.ustc.edu.cn
Received: December 10, 2024; Accepted: March 06, 2025

Realizing soft two-dimensional room temperature magnets in oxidized $(Fe_{75}Co_{25})_5GeTe_2$

Chunyu Qin[1], Yanan Yuan[1], Jiapeng Zhao[2], Daxiang Liu[1], Fangfang Pei[1], Siyu Wang[1], Xiaoli Chen[1], Xiang Chen[3], Hongrui Zhang[4], Mengmeng Yang[5], He Huang[2] ✉, and Qian Li[1] ✉

[1]*National Synchrotron Radiation Laboratory, and School of Nuclear Science and Technology, University of Science and Technology of China, Hefei 230029, China;*
[2]*School of Materials Science and Engineering, University of Science and Technology Beijing, Beijing 100083, China;*
[3]*Center for Neutron Science and Technology, Guangdong Provincial Key Laboratory of Magnetoelectric Physics and Devices, School of Physics, Sun Yat-Sen University, Guangzhou 510275, China;*
[4]*Ningbo Institute of Materials Technology & Engineering, Chinese Academy of Sciences, Ningbo 315201, China;*
[5]*Anhui Key Laboratory of Magnetic Functional Materials and Devices, Institute of Physical Science and Information Technology, Anhui University, Hefei 230601, China*

✉Correspondence: He Huang, E-mail: hhuang@ustb.edu.cn; Qian Li, E-mail: liqian89@ustc.edu.cn

Cite This: *JUSTC*, **2025**, 55(10): 1004 (7pp)   Read Online   Supporting Information

Abstract: Two-dimensional (2D) van der Waals (vdW) magnets have demonstrated intriguing functionalities in spintronic devices and have drawn enormous interest. Nevertheless, the development of soft in-plane 2D magnets with low coercivity remains limited. In this study, we fabricated a high-quality $(Fe_{75}Co_{25})_5GeTe_2$ crystal and achieved a soft in-plane 2D magnet with coercivity of approximately 3 Oe in a naturally oxidized $(Fe_{75}Co_{25})_5GeTe_2$ flake at room temperature. A combination of X-ray magnetic circular dichroism (XMCD) and ferromagnetic resonance (FMR) revealed a high Curie temperature of ~350 K and relatively low magnetic damping at room temperature. Kerr microscopy further demonstrated that the oxidized flakes exhibited exchange bias and an unconventional reduction in coercivity compared with their non-oxidized counterparts at liquid nitrogen temperatures. Detailed analyses using transmission electron microscopy (TEM) and density functional theory (DFT) calculations attribute this behavior to modifications in magnetic anisotropy and interlayer exchange coupling induced by oxygen intercalation. These findings deepen the understanding of the magnetic properties of the cobalt-doped Fe_5GeTe_2 family and highlight the potential of oxidation modulation in 2D vdW magnets, positioning $(Fe_{75}Co_{25})_5GeTe_2$ as a promising candidate for next-generation spintronic devices.

Keywords: soft two-dimensional van der Waals ferromagnet; exchange bias; X-ray magnetic circular dichroism; Kerr microscopy; ferromagnetic resonance

CLC number: O469   **Document code:** A

1 Introduction

The recent advent of two-dimensional (2D) magnetism in exfoliatable van der Waals (vdW) materials has garnered significant attention in both fundamental and applied research[1,2]. These 2D vdW magnetic materials exhibit unique features, including ideal morphologies, well-defined atomic-level vdW interfaces, weak vdW interfacial exchange coupling, high surface-to-volume ratios, and exceptional mechanical flexibility. These attributes make them promising candidates for next-generation spintronic devices[3]. Great efforts have been dedicated to increasing the Curie temperature (T_C) of vdW magnets to room temperature (RT) and beyond while simultaneously modulating their magnetic properties[4]. Strategies such as the application of high pressure[5], strain[6], and magnetic proximity effect[7] have proven effective in dramatically increasing the T_C and altering magnetic anisotropy. Additionally, the intercalation of foreign atoms, including Li^+[8], protons[9], oxygen[10], and Ga^+[11–13], has demonstrated remarkable success in increasing the T_C and enabling gate-controlled phase transitions.

Among layered vdW magnetic materials, the Fe_nGeTe_2 (n = 3, 4, 5) family stands out because of its high intrinsic T_C and versatile tunability of its magnetic properties[4]. Increasing the Fe content from n = 3 to n = 5 raises T_C from 220–230 K, with a saturation magnetization of ~376 emu/cm^3[11,14,15], to 270–330 K, with a saturation magnetization of 500–640 emu/cm^3[16–19]. Partial substitution of Fe with Ni in $(Fe_{1-x}Ni_x)_5GeTe_2$ has been reported to achieve a record-high T_C of 478 K[20]. Similarly, Co substitution in Fe_5GeTe_2 (up to 30%) not only enhances T_C but also reorients the magnetic easy axis from out-of-plane [001] axis to in-plane direction[21–24]. Higher cobalt doping levels (34% to 55%) induce a transition in $(Fe_{1-x}Co_x)_5GeTe_2$ from ferromagnetic to antiferromagnetic behavior[21–25]. Recent studies have demonstrated the potential of $(Fe_{0.85}Co_{0.15})_5GeTe_2$ with strong in-plane room temperature magnetization and spin polarization in spin valve devices as an efficient spin injection and detection layer[26]. Notably, monolayer flakes of $(Fe_{0.56}Co_{0.44})_5GeTe_2$ have shown

CSTR: 32290.14.JUSTC-2024-0153
DOI: 10.52396/JUSTC-2024-0153
JUSTC, **2025**, 55(10): 1004

record-high RT ferromagnetic order[27]. Despite these advancements, the modulation of soft in-plane magnetism in $(Fe_{1-x}Co_x)_5GeTe_2$ remains underexplored. Soft in-plane ferromagnets are particularly valuable for unconventional neuromorphic computing[28,29] and probabilistic computing[30]. Their small coercivity and low hysteresis loss make them highly promising for spintronic memory devices.

Ambient oxidation has emerged as an effective method to modulate the magnetic properties of 2D magnets, leading to a range of intriguing phenomena, including exchange bias[10,31–33], unusual hysteresis loop shapes[34], and oxidation-dependent magnetic domains and skyrmions[35,36]. In this study, we synthesized high-quality 25% Co doped Fe_5GeTe_2 crystals, denoted as $(Fe_{75}Co_{25})_5GeTe_2$ (FCGT). Kerr microscopy and X-ray magnetic circular dichroism (XMCD) measurements revealed a high Curie temperature (~350 K) for FCGT. Notably, naturally oxidized FCGT flakes exhibited exchange bias and an unconventionally smaller coercivity than freshly exfoliated (non-oxidized) flakes at liquid nitrogen temperature. The oxidized FCGT demonstrated a small coercivity of ~3 Oe and relatively low Gilbert damping at room temperature, highlighting its strong potential for applications in 2D magnet-based spintronic devices.

2 Materials and methods

The $(Fe_{75}Co_{25})_5GeTe_2$ crystal was synthesized via the chemical vapor transport method. As depicted in Fig. 1a, the FCGT structure consists of a covalently bonded $(FeCo)_5Ge$ slab sandwiched between two Te layers. The material adopts a rhombohedral $R\bar{3}m$ structure, featuring five distinct Fe(Co) atomic sites, where Co atoms are known to substitute for Fe atoms upon doping. High-resolution cross-sectional scanning transmission electron microscopy (TEM) images of the ac-plane (Fig. 2), along with sharp electron diffraction patterns (inset of Fig. 2b), confirm the high quality of the synthesized single-crystalline FCGT samples. The TEM analysis reveals lattice parameters of approximately 0.990 nm along the *c*-axis and 0.402 nm along the *a*-axis, which are comparable to the values reported in Ref. [22]. Furthermore, energy dispersive X-ray (EDX) spectroscopy mapping (Fig. 1c) demonstrated

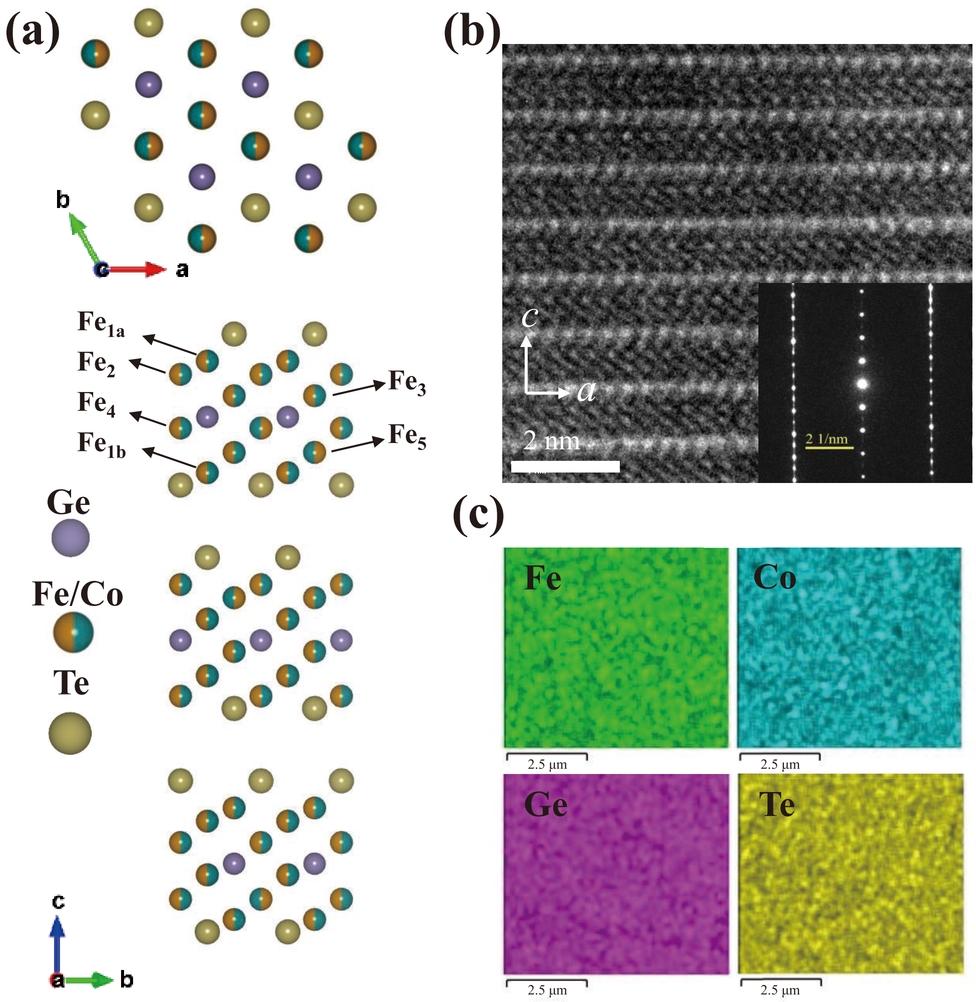

Fig. 1. (a) Schematic illustration of the atomic structure of $(Fe_{1-x}Co_x)_5GeTe_2$ from the top view and side view. (b) High-resolution cross-sectional scanning TEM images of the ac plane of $(Fe_{75}Co_{25})_5GeTe_2$. The inset shows the corresponding electron diffraction patterns. (c) EDX mapping of $(Fe_{75}Co_{25})_5GeTe_2$, suggesting a uniform distribution of constituent elements.

CSTR: 32290.14.JUSTC-2024-0153
DOI: 10.52396/JUSTC-2024-0153
JUSTC, **2025**, 55(10): 1004

the uniform distribution of the constituent elements in the FCGT crystal. The atomic ratios of Fe ∶ Co ∶ Ge ∶ Te were determined to be 4.35 ∶ 1.42 ∶ 1 ∶ 1.95, corroborating the expected stoichiometry.

The GHz dynamic magnetic properties of FCGT were investigated using a custom-built ferromagnetic resonance (FMR) system. A coplanar waveguide (CPW) with a 50 Ω impedance was employed to deliver the microwave field to the sample. The FCGT crystal was placed directly onto the CPW, with measurements performed in an in-plane magnetic field geometry. For each microwave frequency, a high magnetic field was initially applied to fully saturate the sample's magnetization. The magnetic field was subsequently swept from a high positive value to a high negative value. At each magnetic field step, a microwave signal generator and a diode detector were used to measure the power absorbed by the sample. To enhance the signal-to-noise ratio, a small modulated magnetic field was applied in combination with a lock-in amplifier.

Hysteresis loops in this study were measured using a commercial Kerr microscopy system (Tuotuo Technology) with a light source wavelength of 620 nm. Low-temperature measurements were conducted in a cryostat cooled by liquid nitrogen flow. For the hysteresis loop measurement presented in Fig. 3, a long working distance 50× objective with a numerical aperture (NA) of 0.42 was employed. The incident light was at a grazing angle (~24.8° relative to the normal direction) while the magnetic field was applied in the plane of the sample (see Fig. S2a in Supporting information).

First-principle calculations in this study were performed using density functional theory (DFT) as implemented in the Vienna ab initio simulation package (VASP). The exchange–correlation interactions were modeled using the Perdew–Burke–Ernzerhof (PBE) functional within the generalized gradient approximation (GGA) framework. The first Brillouin zone was sampled using an 11 × 11 × 2 grid of gamma-centered *k*-points. A plane-wave energy cutoff of 520 eV was employed. During the atomic optimization, the Hellman–Feynman force tolerance was set to 0.03 eV/Å, and the energy convergence criterion was 10^{-5} eV. Spin–orbit coupling (SOC) was included in the calculations to determine the magnetic anisotropy energy (MAE), defined as the energy difference between the magnetization easy axis along the [100] and [001] crystallographic directions. Considering the similar magnetic behavior with Co doping of less than 30% in Fe_5GeTe_2[21,22], a slightly different element ratio from experimental samples was used to simplify the calculation.

3 Results and discussion

To investigate the GHz dynamic magnetic properties of FCGT, FMR measurements were performed. During the FMR measurement, the fabricated FCGT crystal was placed on a coplanar waveguide with an in-plane magnetic field applied along the signal line of waveguide. This configuration allows the GHz microwave-generated alternating magnetic field to excite magnetization precession, enabling the interaction between microwave signal and magnetization dynamics to be probed. Fig. 2a shows the FMR spectra of FCGT at various microwave frequencies at room temperature (RT), confirming the ferromagnetic state of FCGT at RT. By fitting the FMR spectra with a combination of symmetric and antisymmetric Lorentzian functions, the resonance field H_r and peak-to-peak ΔH were extracted as a function of microwave frequency, as depicted in Fig. 2b and c.

The resonance field versus microwave frequency curve (Fig. 2b) was fitted with the Kittel equation[13,37]:

$$f = \gamma' \sqrt{(H_r + 4\pi M_{\text{eff}})H_r}, \tag{1}$$

where f is the microwave frequency, $\gamma' = \frac{\gamma}{2\pi}$ is the reduced gyromagnetic ratio, and $4\pi M_{\text{eff}}$ is the effective magnetization. Fitting the data in Fig. 2b with Eq. (1) yielded a Landé g-factor of 2.296, using $|\gamma| = g\frac{\mu_B}{\hbar}$ and the effective magnetization $4\pi M_{\text{eff}}$ value of 2.201 kG, which is consistent with Ref. [37] results. In Fig. 2c, the linewidth ΔH shows the expected linear dependence on frequency f, with the slope α representing the effective FMR damping[13,37]:

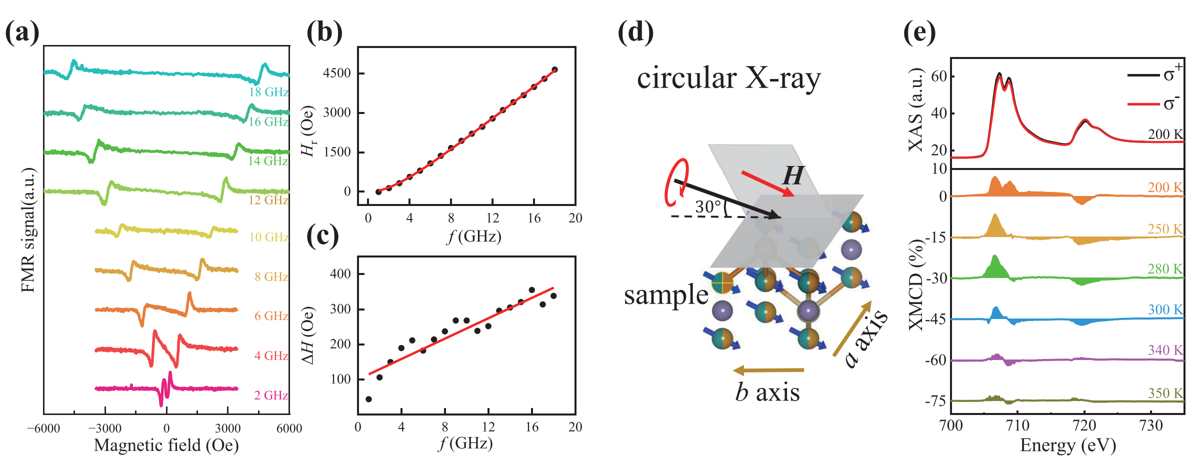

Fig. 2. (a) Frequency-dependent ferromagnetic resonance spectra with a magnetic field applied along the in-plane direction of $(Fe_{75}Co_{25})_5GeTe_2$. Summary of (b) resonance fields and (c) linewidth as a function of frequency. The solid red lines are fitting curves using Eqs. (1) and (2), respectively. (d) Schematic drawing of the X-ray magnetic circular dichroism measurement geometry, with circularly polarized X-rays at grazing incident angle and magnetic field of 0.2 T along X-ray direction. (e) Typical X-ray absorption spectra and temperature-dependent XMCD spectra.

CSTR: 32290.14.JUSTC-2024-0153
DOI: 10.52396/JUSTC-2024-0153
JUSTC, **2025**, 55(10): 1004

$$\Delta H = \frac{2\alpha_{\text{eff}}}{\sqrt{3}|\gamma|}\frac{f}{2\pi} + \Delta H_0 + \Delta H_{\text{TMS}}, \tag{2}$$

where ΔH_0 is the intercept of the linewidth at zero frequency, ΔH_{TMS} accounts for two-magnon scattering, and γ is the gyromagnetic ratio. The linear fit (solid lines) of Fig. 2c yields α = 0.040 for FCGT with external magnetic field applied along the in-plane direction. These FMR results indicate that the bulk FCGT crystal maintains RT magnetism and spin dynamics under the influence of high-frequency microwaves.

Next, we characterized the electronic and spin structure of FCGT using the element-resolved X-ray magnetic circular dichroism (XMCD) at Fe L edge. As shown in Fig. 2d, XMCD measurements were performed with circularly polarized X-rays at grazing incidence, where a magnetic field of 0.2 T was applied along the X-ray direction. The angle between sample surface and X-ray incidence direction was set to 30° to balance the spot size of X-ray on sample and the projection of the sample's magnetization along the X-ray direction. Fig. 2e displays a typical X-ray absorption spectroscopy (XAS) of FCGT with left (σ^+) and right (σ^-) circularly polarized X-rays. The XMCD signal is obtained by taking the difference between the two spectra, where a nonzero XMCD signal indicates the presence of a magnetic moment of Fe atoms in FCGT. We observed that the amplitude of XMCD signal decreased with increasing temperature and completely vanished at approximately 350 K, clearly indicating the Curie temperature of FCGT was approximately 350 K. According to previous theoretical calculations[21] and photoemission electron microscopy images[27] from Co doped Fe_5GeTe_2, the coupling between Fe spin and Co spin was ferromagnetic.

As previously noted, the ambient oxidation strategy has led to the observation of many intriguing phenomena in 2D vdW magnets[31–36]. In this study, prior to applying the oxidation strategy, we first fabricated a freshly exfoliated 480 nm-thick FCGT flake (see Supporting information Fig. S1). To avoid any inadvertent oxidation, the fresh FCGT sample was loaded onto a cryostat for low-temperature Kerr microscopy measurement within the inert atmosphere of a glove box. The sample was measured in longitudinal magneto-optic Kerr effect mode, with magnetic field applied along the ab-plane of FCGT (Fig. S2a). As shown in Fig. 3a, the non-oxidized FCGT flake exhibited a square-shaped easy-axis hysteresis loop at liquid nitrogen temperature, indicating an in-plane easy axis of magnetization. The coercivity decreased from ~23.3 Oe to ~7.75 Oe at RT (Fig. 3b), which can be attributed to the weakened magnetic anisotropy at higher temperatures. We subsequently adopted the oxidation strategy by exposing the sample to air for approximately 4 h. As shown in Fig. 3a, the oxidized FCGT flake displayed an unusual narrowed hysteresis loop, with a clear exchange bias of ~−5.64 Oe and a reduced coercivity compared to the non-oxidized sample. Temperature-dependent hysteresis loops in Fig. 3c revealed that the coercivity decreased from ~10.4 Oe at 78 K to ~3.20 Oe at RT and further decreased to ~1.25 Oe at 338 K, demonstrating that the oxidized FCGT is a promising candidate for soft magnet applications. The magnitude of the Kerr signal decreased with increasing temperature and vanished at approximately 358 K, which is consistent with the Curie temperature obtained from the XMCD measurements.

To explore the physical origin of the unconventional behavior observed in the oxidized FCGT sample, we first employed focused ion beam (FIB) cutting to prepare the sample for cross-sectional imaging using transmission electron microscopy (TEM). Fig. 3d presents a cross-sectional TEM image of the oxidized FCGT sample, which consists of two distinct regions: the top ~2.5 nm of oxidized FCGT (referred

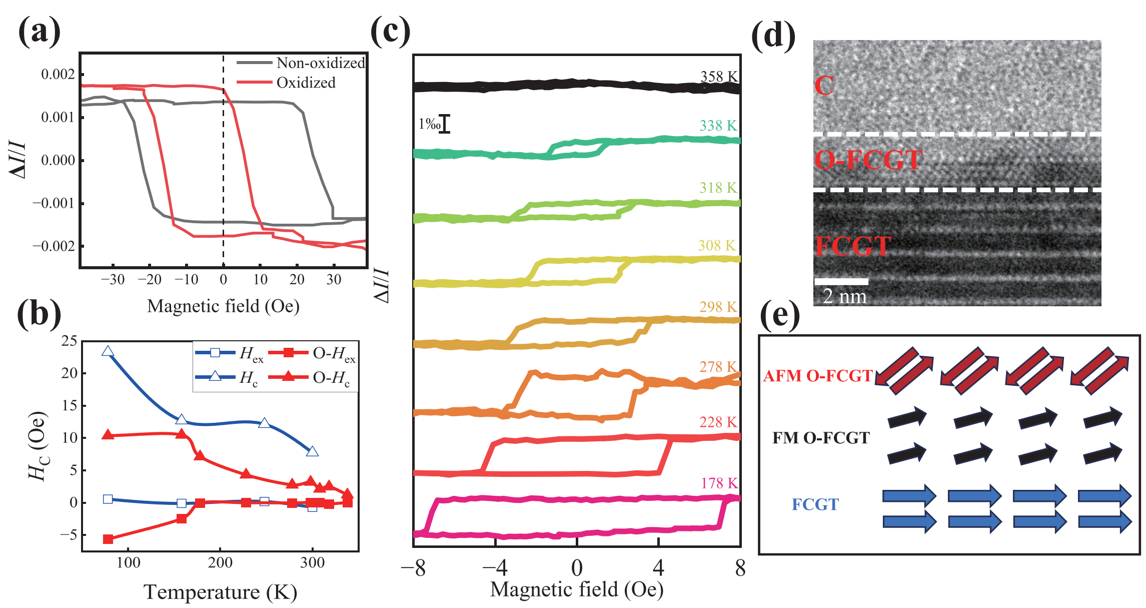

Fig. 3. (a) Hysteresis loops from a freshly-exfoliated FCGT nanoflake before and after oxidization. (b) Summary of the exchange bias field and coercivity field from pristine and oxidized FCGT as a function of temperature. (c) Hysteresis loops from oxidized FCGT as a function of temperature. (d) Cross-sectional scanning TEM image of oxidized sample clearly shows the formation of oxidized FCGT on top of the pristine FCGT. (e) Schematic drawing of the model in our oxidized FCGT sample, which consists of two parts of O-FCGT and FCGT. A formation of exchange spring spin structure at interface was speculated from the exchange coupling between a ferromagnet with in-plane easy axis and an antiferromagnet with out-of-plane easy axis.

CSTR: 32290.14.JUSTC-2024-0153
DOI: 10.52396/JUSTC-2024-0153
JUSTC, **2025**, 55(10): 1004

to as O-FCGT) and the bottom FCGT layer. The bottom FCGT region maintained its pristine single-crystalline structure, with a clear vdW gap, while the top oxidized FCGT (O-FCGT) region displayed a degraded crystalline structure, lacking the vdW gap between the Te atoms. Notably, the portion of O-FCGT closer to the bottom FCGT exhibited a relatively better crystalline quality, likely due to a lower degree of oxidation. Based on these observations, we consider the oxidized FCGT sample to consist of three parts, as illustrated in the schematic drawing of Fig. 3e.

To explore the type of interlayer exchange coupling and the strength of magnetic anisotropy as a function of oxygen intercalation, we performed density functional theory (DFT) calculations on Fe_5GeTe_2, 20% Co doped Fe_5GeTe_2, and oxygen-intercalated $(Fe_4Co)_5GeTe_2$. Two scenarios of oxygen intercalation in $(Fe_4Co)_5GeTe_2$ were simulated: $(Fe_4Co)_5GeTe_2$-1O (one oxygen atom intercalated per unit cell) and $(Fe_4Co)_5GeTe_2$-2O (two oxygen atoms intercalated per unit cell). Based on the DFT calculation results in Fig. 4b, both Fe_5GeTe_2 and $Fe_4CoGeTe_2$ exhibit a ferromagnetic (FM) type of interlayer coupling. While Fe_5GeTe_2 exhibits an out-of-plane easy axis of magnetization, $Fe_4CoGeTe_2$ has an in-plane easy axis of magnetization (Fig. 4c). These results are consistent with previous reports on Fe_5GeTe_2 and Co doped Fe_5GeTe_2[15,16,18,20–26], especially given that the simulation was performed at zero temperature for thin Fe_5GeTe_2. Moreover, as shown in Fig. 4a, our DFT calculations indicate that oxygen intercalation results in an antiferromagnetic (AFM) type of interlayer coupling (Fig. 4b) and an out-of-plane oriented easy axis of magneto-crystalline anisotropy in O-intercalated FCGT (Fig. 4c). Despite the calculated out-of-plane magnetic anisotropy for O-FCGT, the spins of O-FCGT are expected to be canted, with both in-plane and out-of-plane components, due to the exchange coupling between the in-plane magnetized FCGT and the AFM phase of O-FCGT. Therefore, the appearance of exchange bias (Fig. 3a) in oxidized FCGT can be attributed to the pinning effect of the in-plane component of the AFM-ordered layer in O-FCGT.

In non-vdW FM/AFM bilayer films, the appearance of exchange bias is typically accompanied by an increase in coercivity due to the additional energy required to switch the rotatable AFM spins[38,39]. However, as shown in Fig. 3a, we observed a clear reduction in coercivity after applying the oxidation strategy. The behavior of reduced coercivity and enhanced Kerr signal from O-FCGT sample, compared to the same sample before oxidation, is also demonstrated in Fig. S2b. Considering the gradient of oxygen diffusion in O-FCGT[10,33–35], the crystalline structure, as confirmed by the cross-sectional scanning TEM images of oxidized sample in Fig. 3d and magnetic state in the O-FCGT layer should not be homogeneous. Thus, we speculate that O-FCGT layer consists of two distinct regions: one with AFM-ordered O-FCGT and the other with FM-ordered O-FCGT exhibiting weak magnetic anisotropy (Fig. 3e). Unfortunately, DFT calculations for O-intercalated FCGT with an oxygen concentration lower than 1O (one oxygen atom intercalated per unit cell) are not technically feasible. However, our previous work[10] on oxygen-intercalated Fe_3GaTe_2 demonstrated that even small concentration levels of oxygen intercalation into the vdW magnet can induce an FM-ordered phase. The nearly square-shaped easy-axis hysteresis loops in Fig. 3a and magnetic domain images during field scanning (Fig. S3) suggest that the in-plane magnetization reversal mode follows a

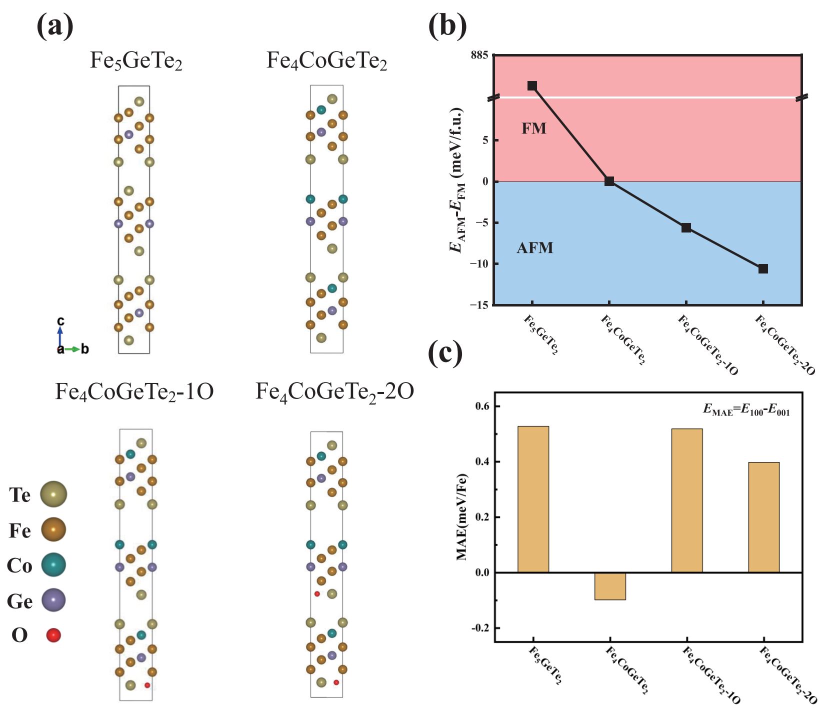

Fig. 4. (a) Schematic drawing of Fe_5GeTe_2, Co doped Fe_5GeTe_2, and oxidized $Fe_4CoGeTe_2$ with different concentrations of intercalated O. Density functional theory (DFT) calculation result of (b) energy difference between ferromagnetic (FM) and antiferromagnetic (AFM) alignment of interlayer spins and (c) magneto-crystalline anisotropy of four situations shown in (a).

CSTR: 32290.14.JUSTC-2024-0153
DOI: 10.52396/JUSTC-2024-0153
JUSTC, **2025**, 55(10): 1004

combination of initial domain nucleation and subsequent domain wall propagation. In this reversal mode, the coercivity is primarily dominated by nucleation field mechanism[40]. It is possible that the FM-ordered O-FCGT, which nucleated at a smaller magnetic field, lowered the critical field required for the nucleation of the bottom FCGT layer, thereby significantly reducing the coercivity. The enhanced Kerr signal in oxidized FCGT could be attributed to the reflection at the emerging O-FCGT/FCGT interfaces[41] or the different magneto-optical response of FM-ordered O-FCGT compared to FCGT.As revealed in previous studies of oxidized vdW magnets[10,33–35], the amorphous crystal structure and nonuniform chemical composition make the characterization of magnetic order in the oxidized layer particularly challenging. Although further characterization and investigation are needed for the oxidized FCGT flakes, our intriguing results demonstrate that ambient oxidation provides an efficient route to create soft 2D vdW magnets.

4 Conclusions

In conclusion, we successfully fabricated high-quality $(Fe_{75}Co_{25})_5GeTe_2$ crystal and realized a soft in-plane room temperature 2D magnet with a coercivity of approximately 3 Oe in the naturally oxidized $(Fe_{75}Co_{25})_5GeTe_2$ flake. This material exhibits high-frequency ferromagnetic resonance with relatively low damping. Our results not only enrich the understanding of magnetic properties in the 2D vdW magnet family, particularly for cobalt doped Fe_5GeTe_2, but also reveal the intriguing effects of oxidation modulation on 2D vdW magnets. Our discovery of room-temperature soft 2D magnetism in $(Fe_{75}Co_{25})_5GeTe_2$ coupled with high-frequency spin dynamics suggests that this material is a promising candidate for future 2D magnet-based spintronic devices.

Supporting information

The supporting information for this article can be found online at https://doi.org/10.52396/JUSTC-2024-0153. The supporting information includes three figures showing the optical image, AFM characterization of FCGT flake, schematic drawing of Kerr measurement geometry and comparison of hysteresis loops from another flake, and magnetic domain images observed by Kerr microscope at different temperatures.

Acknowledgements

The work was supported by the National Key Research and Development Program of China (2023YFA1406400), the National Natural Science Foundation of China (12174364, 52201288, 12104003, 12241406), the Fundamental Research Funds for the Central Universities (WK2310000104), the USTC Research Funds of the Double First-Class Initiative (YD2140002004), and the Natural Science Foundation of Anhui Province (2308085Y04). This work was partially carried out at the USTC Center for Micro and Nanoscale Research and Fabrication. This research used resources of Beamlines XMCD-A and XMCD-B (Soochow Beamline for Energy Materials) at NSRL. The XAS and XMCD measurements were performed at the vector magnet endstation at BL07U at Shanghai Synchrotron Radiation Facility (SSRF) and beamline XMCD-a at NSRL.

Conflict of interest

The authors declare that they have no conflict of interest.

Biographies

Chunyu Qin is a graduate student studying in the National Synchrotron Radiation Laboratory, University of Science and Technology of China. His research mainly focuses on orbital phenomena in thin films.

He Huang is a Professor at the School of Materials Science and Engineering, University of Science and Technology Beijing. He received his Ph.D. degree from the Hong Kong University of Science and Technology in 2019. His research mainly focuses on using density functional theory to calculate the magnetic properties of two-dimensional van der Waals magnets.

Qian Li is a Professor at the National Synchrotron Radiation Laboratory and School of Nuclear Science and Technology, University of Science and Technology of China. She received her Ph.D. degree from Fudan University in 2015. Her research mainly focuses on modulation of magnetic properties of two-dimensional van der Waals magnets and development of synchrotron radiation-based techniques.

References

[1] Huang B, Clark G, Navarro-Moratalla E, et al. Layer-dependent ferromagnetism in a van der Waals crystal down to the monolayer limit. *Nature*, **2017**, *546*: 270–273
[2] Gong C, Li L, Li Z, et al. Discovery of intrinsic ferromagnetism in two-dimensional van der Waals crystals. *Nature*, **2017**, *546* (7657): 265–269.
[3] Mak K F, Shan J, Ralph D C. Probing and controlling magnetic states in 2D layered magnetic materials. *Nature Reviews Physics*, **2019**, *1*: 646–661.
[4] Wang Q H, Bedoya-Pinto A, Blei M, et al. The magnetic genome of two-dimensional van der Waals materials. *ACS Nano*, **2022**, *16*: 6960–7079.
[5] Li Z, Tang M, Huang J, et al. Magnetic anisotropy control with Curie temperature above 400 K in a van der Waals ferromagnet for spintronic device. *Advanced Materials*, **2022**, *34*: 2201209.
[6] Wang Y, Wang C, Liang S J, et al. Strain-sensitive magnetization reversal of a van der Waals magnet. *Advanced Materials*, **2020**, *32*: 2004533.
[7] Wang H, Liu Y, Wu P, et al. Above room-temperature ferromagnetism in wafer-scale two-dimensional van der Waals Fe_3GeTe_2 tailored by a topological insulator. *ACS Nano*, **2020**, *14*: 10045–10053.
[8] Deng Y, Yu Y, Song Y, et al. Gate-tunable room-temperature ferromagnetism in two-dimensional Fe_3GeTe_2. *Nature*, **2018**, *563*: 94–99.
[9] Zheng G, Xie W Q, Albarakati S, et al. Gate-tuned interlayer coupling in van der Waals ferromagnet Fe_3GeTe_2 nanoflakes. *Physical Review Letters*, **2020**, *125*: 047202.
[10] Liu D, Pei F, Wang S, et al. Manipulation of exchange bias in two-dimensional van der Waals ferromagnet near room temperature. *ACS Nano*, **2024**, *18*: 23812–23822.
[11] Li Q, Yang M, Gong C, et al. Patterning-induced ferromagnetism of Fe_3GeTe_2 van der Waals materials beyond room temperature. *Nano Letters*, **2018**, *18*: 5974–5980.
[12] Yang M, Li Q, Chopdekar R V, et al. Highly enhanced curie temperature in Ga-implanted Fe_3GeTe_2 van der Waals material.

Advanced Quantum Technologies, **2020**, *3*: 2000017.
[13] Yuan Y, Liu D, Yu J, et al. Modulating above-room-temperature magnetism in Ga-implanted Fe_5GeTe_2 van der Waals magnets. *APL Materials*, **2023**, *11*: 091101.
[14] Fei Z, Huang B, Malinowski P, et al. Two-dimensional itinerant ferromagnetism in atomically thin Fe_3GeTe_2. *Nature Materials*, **2018**, *17*: 778–782.
[15] Tan C, Lee J, Jung S G, et al. Hard magnetic properties in nanoflake van der Waals Fe_3GeTe_2. *Nature Communications*, **2018**, *9*: 1554.
[16] May A F, Bridges C A, McGuire M A. Physical properties and thermal stability of $Fe_{5-x}GeTe_2$ single crystals. *Physical Review Materials*, **2019**, *3* (10): 104401.
[17] May A F, Ovchinnikov D, Zheng Q, et al. Ferromagnetism near room temperature in the cleavable van der waals crystal Fe_5GeTe_2. *ACS Nano*, **2019**, *13*: 4436–4442.
[18] Seo J, Kim D Y, An E S, et al. Nearly room temperature ferromagnetism in a magnetic metal-rich van der Waals metal. *Science Advances*, **2020**, *6*: eaay8912.
[19] Zhang H, Chen R, Zhai K, et al. Itinerant ferromagnetism in van der Waals $Fe_{5-x}GeTe_2$ crystals above room temperature. *Physical Review B*, **2020**, *102* (6): 064417.
[20] Chen X, Shao Y T, Chen R, et al. Pervasive beyond room-temperature ferromagnetism in a doped van der Waals magnet. *Physical Review Letters*, **2022**, *128*: 217203.
[21] May A F, Du M H, Cooper V R, et al. Tuning magnetic order in the van der Waals metal Fe_5GeTe_2 by cobalt substitution. *Physical Review Materials*, **2020**, *4*: 074008.
[22] Tian C, Pan F, Xu S, et al. Tunable magnetic properties in van der Waals crystals $(Fe_{1-x}Co_x)_5GeTe_2$. *Applied Physics Letters*, **2020**, *116*: 202402.
[23] Ohta T, Kurokawa K, Jiang N, et al. Enhancement of spin–flop-induced magnetic hysteresis in van der Waals magnet $(Fe_{1-x}Co_x)_5GeTe_2$. *Applied Physics Letters*, **2023**, *122* (15): 152402.
[24] Zhang J, Wang Z, Xing Y, et al. Enhanced magnetic and electrical properties of Co-doped Fe_5GeTe_2. *Applied Physics Letters*, **2024**, *124*: 103103.
[25] Chen X, Schierle E, He Y, et al. Antiferromagnetic order in Co-doped Fe_5GeTe_2 probed by resonant magnetic X-ray scattering. *Physical Review Materials*, **2022**, *6*: 094404.
[26] Ngaloy R, Zhao B, Ershadrad S, et al. Strong in-plane magnetization and spin polarization in $(Co_{0.15}Fe_{0.85})_5GeTe_2$/graphene van der Waals heterostructure spin-valve at room temperature. *ACS Nano*, **2024**, *18*: 5240–5248.
[27] Lu L, Wang Q, Duan H, et al. Tunable magnetism in atomically thin itinerant antiferromagnet with room-temperature ferromagnetic order. *Nano Letters*, **2024**, *24*: 5984–5992.
[28] Cao Y, Rushforth A, Sheng Y, et al. Tuning a binary ferromagnet into a multistate synapse with spin–orbit-torque-induced plasticity. *Advanced Functional Materials*, **2019**, *29*: 1808104.
[29] Marković D, Daniels M W, Sethi P, et al. Easy-plane spin Hall nano-oscillators as spiking neurons for neuromorphic computing. *Physical Review B*, **2022**, *105*: 014411.
[30] Gan C K, Chen B, Zeng M. In-plane dominant anisotropy stochastic magnetic tunnel junction for probabilistic computing: A Fokker–Planck study. *Journal of Magnetism and Magnetic Materials*, **2023**, *586*: 171197.
[31] Gweon H K, Lee S Y, Kwon H Y, et al. Exchange bias in weakly interlayer-coupled van der waals magnet Fe_3GeTe_2. *Nano Letters*, **2021**, *21*: 1672–1678.
[32] Wu Y, Wang W, Pan L, et al. Manipulating exchange bias in a van der waals ferromagnet. *Advanced Materials*, **2022**, *34*: 2105266.
[33] Wang C, Zhu K, Ma Y, et al. Magnetism control with enhanced hard magnetic temperature in heterostructures based on the van der Waals magnet Fe_5GeTe_2. *Physical Review B*, **2023**, *108*: 094408.
[34] Zhao R, Xu W, Wu Y, et al. Self-modulated magnetism in two-dimensional ferromagnet Fe_3GeTe_2 induced by ambient effects. *ACS Applied Nano Materials*, **2023**, *6*: 20982–20989.
[35] Li Y, Hu X, Fereidouni A, et al. Visualizing the effect of oxidation on magnetic domain behavior of nanoscale Fe_3GeTe_2 for applications in spintronics. *ACS Applied Nano Materials*, **2023**, *6*: 4390–4397.
[36] Park T E, Peng L, Liang J, et al. Néel-type skyrmions and their current-induced motion in van der Waals ferromagnet-based heterostructures. *Physical Review B*, **2021**, *103*: 104410.
[37] Alahmed L, Nepal B, Macy J, et al. Magnetism and spin dynamics in room-temperature van der Waals magnet Fe_5GeTe_2. *2D Materials*, **2021**, *8*: 045030.
[38] Nogués J, Schuller I K. Exchange bias. *Journal of Magnetism and Magnetic Materials*, **1999**, *192*: 203–232.
[39] Kiwi M. Exchange bias theory. *Journal of Magnetism and Magnetic Materials*, **2001**, *234*: 584–595.
[40] Guo J J, Xia Q L, Wang X G, et al. Temperature and thickness dependent magnetization reversal in 2D layered ferromagnetic material Fe_3GeTe_2. *Journal of Magnetism and Magnetic Materials*, **2021**, *527*: 167719.
[41] Qiu Z Q, Bader S D. Surface magneto-optic Kerr effect. *Review of Scientific Instruments*, **2000**, *71*: 1243–1255.

CSTR: 32290.14.JUSTC-2024-0153
DOI: 10.52396/JUSTC-2024-0153
JUSTC, **2025**, 55(10): 1004